Electro-Optic Imaging Fourier Transform Spectrometer

Tien-Hsin Chao, Hanying Zhou,
Jet Propulsion Laboratory
4800 Oak Grove Drive, Pasadena CA, 91109

Xiaowei Xia, Steve Serati
Boulder Nonlinear Systems Inc.
450 Courtney Way, #107, Lafayette, CO 80026

Abstract-JPL is developing an innovative compact, low mass, Electro-Optic Imaging Fourier Transform Spectrometer (E-O IFTS) for hyperspectral imaging applications. The spectral region of this spectrometer will be 1 – 2.5 μm (1000 – 4000 cm^{-1}) to allow high-resolution, high-speed hyperspectral imaging applications. The specific applications for NASA's missions will focus on the measurement of a large number of different atmospheric gases simultaneously in the same airmass. Due to the use of a combination of birefringent phase retarders and multiple achromatic phase switches to achieve phase delay, this spectrometer is capable of hyperspectral measurements similar to that of the conventional Fourier transform spectrometer but without any moving parts. In this paper, the principle of operations, system architecture and recent experimental progress will be presented.

I. Introduction

Traditional Fourier transform spectrometers possess two major advantages over grating, prism, and circular variable filter (CVF) spectrometers. One is the time-multiplexing effect. The Michelson interferometer's single detector views all the wavelengths (within the sensor passband) simultaneously throughout the entire measurement. This effectively lets the detector collect data on each wavelength for the entire measurement time, measuring more photons and therefore, results in higher signal-to-noise ratio, at best for situations where the source is stable. The other is the throughout advantages since the FTS does not need spatial filters (e.g. slit) in the optical light path.

However, Traditional FTIR spectrometers, used in space flight missions, obtain their optical delay by physically translating one or more optical components. The so-called translation mechanism usually dominates the risk, cost, power consumption, and performance of such instruments because:

1) Over the course of a 5-year mission, tens of millions of strokes will be required, making wear or fatigue a serious risk

2) The moving optical element cannot be rigidly held, making it sensitive to vibration and requiring that it be "caged" during launch to prevent damage, adding risk (failure of the caging mechanism to reopen).

3) Accelerating and decelerating the optical elements can torque the spacecraft, making it difficult to maintain accurate pointing.

A high-resolution FTIR spectrometer without moving parts therefore represents a substantial improvement in reliability, mission duration, and performance. It also promises to be much smaller in size and mass.

II. Electro-optic imaging fourier transform spectrometer

A. Principle of Operation and System Architecture

This paper describes the design of a novel, high-throughput, liquid-crystal-based IFTS for operation in the infrared spectral band. This approach takes advantage of fast switching ferroelectric or dual-frequency nematic LC modulators to quickly vary the time delay in order to implement fast-acquisition of the time-series data. This on-going effort is an extension of the successful development experience of an IFTS prototype that operated in the visible band (500-800nm) during previous research.

This proposal specifically addresses the need for reducing the weight, size and power consumption of Fourier transform spectrometers (FTS) by eliminating all moving parts. As shown in Figure 1a, in a traditional FTS, the critical time delay data is acquired by scanning one mirror within a Michelson interferometer. Post-processing of the output time measurements using Fast Fourier transform (FFT) will retrieve the spectral data. In the new E-O IFTS, the bulky, slow scanning mechanism is replaced with a solid-state time delay design using Electro-Optic (E-O)

components as shown in Figure 1b. After the input beams passing through a polarizer and a linear retarder made of a birefringent material, the speed difference in refraction indexes between the ordinary and the extraordinary components will generate a time delay in the two throughput beams.

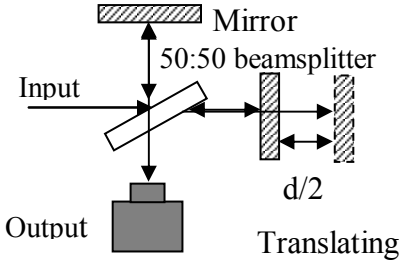

Time Delay: d/c

(a)

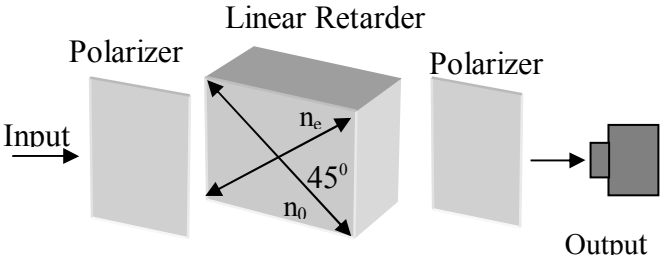

Time Delay: $\frac{(n_e - n_0)d}{c}$

(b)

Figure 1. Time delay mechanisms of (a) a Michelson interferometer based FTS; and (b) an E-O solid-state FTS.

As shown in Figure 2, the E-O FT spectrometer would be built upon a sequence of the time-delay unit. It consists an input polarizer, a passive quarter-wave plates (phase shifter), a series of N liquid crystal based electro-optic switches (S_1, S_2, ..S_n) interlaced with a series of (N+1) passive birefringent wave retarders (Γ_1, Γ_2, .. Γ_{n+1}), as described in figure 1a, and an output polarizer. The basic building block of system is the unit consisting of a single achromatic half-wave switch sandwiched between two neighboring passive wave retarders. The principle is that one can select between the sum or difference in total retardation of the wave passing through these two passive wave retarders by rotating the in-between achromatic half-wave switch. With parallel passive retarders oriented at 45 degrees to the input polarization, an achromatic half-wave retarder oriented at 0-degree gives the difference in retardation, while an orientation of 45 degrees gives the sum. By stacking (n+1) passive retarders, with (n) achromatic half-wave switches between them, the 2^n states of the structure represent all combinations of sums and differences of the retardance values. By using a geometric relationship of passive retarder thickness, an arithmetic progression in time delay steps is achieved**.**

The output of the FTS is a periodic representation of the original bandlimited input spectrum. This periodicity results from the fact that the autocorrelation of the field is sampled to recover the spectrum. Due to the limited number of time-samples, the output spectrum is more accurately a smoothed periodic representation of the input. Knowing this, one can consider the input as a single cycle of the resulting periodic output spectrum. Since the output spectrum is periodic, we can of course express it as a Fourier series

$$S(\omega) = A_0 + \sum_{m=1}^{\infty} A_m \cos(\frac{2\pi m\omega}{\Delta\omega}) + \sum_{m=1}^{\infty} B_m \sin(\frac{2\pi m\omega}{\Delta\omega})$$

where $\Delta\omega$ is the bandwidth of the spectrum and the Fourier coefficients are given below

$$A_0 = \frac{1}{\Delta\omega}\int_{-\frac{\Delta\omega}{2}}^{\frac{\Delta\omega}{2}} S(\omega)d\omega$$

$$A_m = \frac{2}{\Delta\omega}\int_{-\frac{\Delta\omega}{2}}^{\frac{\Delta\omega}{2}} S(\omega)\cos(\frac{2\pi m\omega}{\Delta\omega})d\omega$$

$$B_m = \frac{2}{\Delta\omega}\int_{-\frac{\Delta\omega}{2}}^{\frac{\Delta\omega}{2}} S(\omega)\sin(\frac{2\pi m\omega}{\Delta\omega})d\omega$$

The total power on the detector is the integral of the input spectrum modulated by the transmission function of the FTS

$$P = \int_0^{\infty} S(\omega)T(\omega)d\omega = \frac{1}{2}\int_0^{\infty} S(\omega)d\omega + \frac{1}{2}\int_0^{\infty} S(\omega)\cos(\frac{2\pi m}{\Delta\omega}\omega + \varphi)d\omega$$

Where we have used the transmission function of the FTS that contains active LC switches and multi-order retarders between two polarizers,

$$T = \cos^2(\frac{\Gamma}{2} + \frac{\varphi}{2}),$$

where $\Gamma = \frac{\Delta n d}{c}\omega$ is the phase retardation of the multi-order retarder for one stage, determined by its thickness, *d*, and birefringence, $\Delta n = (n_e - n_0)$, *c* is the speed of

light. φ is a pure phase shift, as provided by an achromatic polarization switch. As described in the above, for fundamental τ_0 according to

$$\Gamma = m\tau_0\omega = \frac{2\pi m}{\Delta\omega}\omega$$

Assume that the achromatic phase shifter φ. switches between four states separated by a quarter-wave of retardation (i.e. φ = -$\frac{\pi}{2}$,0, $\frac{\pi}{2}$ and π), which was done by using the combination of an achromatic half-wave switch (S_{n+1} in Fig. 1) with an achromatic quarter-wave switch (λ/4 in Fig. 1). For one particular multi-order retardance (m), we generate four power measurements on the detector $P_m^0, P_m^\pi, P_m^{\frac{\pi}{2}} and P_m^{\frac{-\pi}{2}}$. Then, in the window of bandwidth, we have

$$P_m^A = P_m^0 - P_m^\pi = \int_0^\infty S(\omega)\cos(\frac{2\pi m\omega}{\Delta\omega})d\omega = \int_{\omega_0-\frac{\Delta\omega}{2}}^{\omega_0+\frac{\Delta\omega}{2}} S(\omega)\cos(\frac{2\pi m\omega}{\Delta\omega})d\omega$$

$$P_0 = P_m^0 + P_m^\pi = P_m^{\frac{\pi}{2}} + P_m^{\frac{-\pi}{2}} = \int_0^\infty S(\omega)d\omega = \int_{\omega_0-\frac{\Delta\omega}{2}}^{\omega_0+\frac{\Delta\omega}{2}} S(\omega)d\omega$$

Compared with the first equation, the spectrum is constructed by assembling the Fourier series using the sequence of power measurements

$$S(\omega) = \frac{1}{\Delta\omega}\left[P_0 + 2\sum_{m=1}^{\infty} P_m^A \cos(\frac{2\pi m\omega}{\Delta\omega}) + 2\sum_{m=1}^{\infty} P_m^B \sin(\frac{2\pi m\omega}{\Delta\omega})\right]$$

This shows that the FTS can, in principle, recover a spectrum. The Fourier coefficients are measured using structures between the polarizers: (1) A digital switch that changes the period of a sinusoidal transmission function in multiples of the input spectral bandwidth, and (2) A four-state achromatic switchable retarder that steps in quarter-wave increments at each order.

The common-path design is physically compact and inherently stable with no moving parts. By replacing precision mechanical movements with low-power binary liquid crystal switches, power supply and packaging requirements are greatly reduced which translates into a large weight reduction. In addition, the common-path approach simplifies the optical design. The in-line optical design reduces size and its mechanical stability and durability. These benefits allow the optical head to be fabricated as a solid block optic with no gaps between elements.

multiple stages, the retardation can be stepped in increments of the

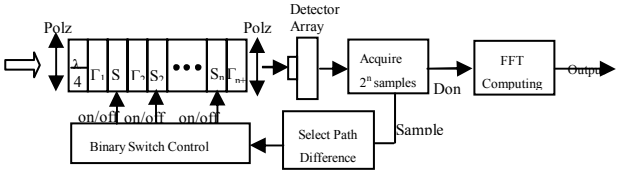

Figure 2. Block diagram of the electro-optic Imaging Fourier transform spectrometer

B. Spectral Resolution

Similar to a conventional FTS, the spectral resolution, $\Delta\sigma$, of the proposed EO-FTS is related to the maximum optical path difference, Δx, or equivalently, the maximum time delay, δ_{max}, between the two interfering waves: (6a) $P_m^B = F$

$$\Delta\sigma = \frac{1}{\Delta x_{\max}} = \frac{1}{d\cdot(n_o - n_e)} = \frac{1}{\lambda\cdot 2^N}. \quad (6b)$$

If a total of N switches (N stages) is used, the time delay of each switch will be approximately $2^0\lambda$, $2^1\lambda$,..., $2^N\lambda$ with maximum time delay $\delta_{max} \sim 2^N\lambda_{med}$ where λ_{med} is the central wavelength of the spectral passband). For the proposed spectrum range of 1.0 ~ 2.5μm, the central wavelength is about 1.8 μm (5500 cm^{-1}). Thus the spectral resolution for an 11-stages and a 13-stages EO-FTS will be about 2.68cm^{-1} and 0.67cm^{-1} respectively.

III. DEVELOPMENT OF A 3-STAGE IR FTS

We have recently developed a 3-stage IRFTS and demonstrated preliminary IR spectral data capture and retrieval. Details of this development work including the fabrication and testing of achromatic half-wave FLC switches, optical design, electronics and software development will be presented. The three-stage IR FTS successfully identified the 1310 nm Diode laser spectrum.

A. Optical Design and Setup

The setup is sketched in Figure 3a. A Diode laser at 1310 nm wavelength was used as light source and a single silica photodiode (*New Focus*, Model#2011) as the light detector. The signal from the detector was acquired by an A/D board in a computer. Multiple optical delays are generated via three achromatic half-wave FLC switches (S1, S2 and S3) put among four passive wave retarders with delays of 1λ, 2λ, 4λ and 8λ respectively. The fourth half-wave switch (S4) was used to generate a 0 or π phase

retardation. An achromatic λ/4 switch was used to shift the system to additional ±π/2 phase. An interface control program was written to apply voltages (±5 V) on the FLC switches, and to acquire signals. Figure 3b shows a photo for the Lab setup of the spectrometer.

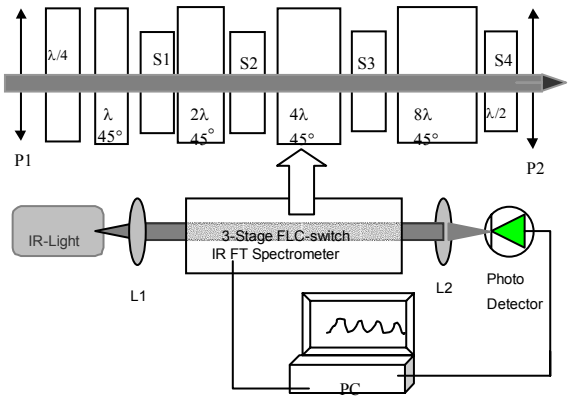

Figure 3a. Schematic setup for the 3-stage spectrometer test.

Figure 3b. Photo of Lab setup for the 3-stage spectrometer.

B. Fabrication of Achromatic Half-Wave Switches

The schematic of the achromatic half-wave solid-state switch is shown in Figure 4. Two passive Nitto Denko retardation film (NRF) sheets and one FLC switch were used to construct the compound retarder. The retardance for each NRF is a full-wave at 600 nm. The retardance of the FLC switch is a half-wave at 1120nm. Four achromatic switches have been fabricated.

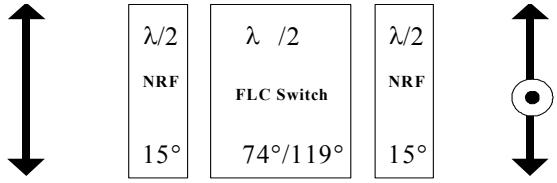

Figure 4. The Schematic of an achromatic half-wave switch

A typical test result (green solid curve) is shown in Figure 5, compared with the simulation results (red dotted curve). During experimental measurements, the LC switch was toggled at a rate of 0.4 Hz, with a driving voltage of ±4.8V. The switch speed of the modulator can be fast, on the order of 100 μs, with low operating voltages (<5V). The spectral range with leakage less than 0.5% is from 0.93 μm to 1.43 μm. The simulation parameters used are: full-wave retardance for each NRF at 600 nm, half-wave retardance of the FLC switch at 1220 nm, and the orientations of the three waveplates at 15°, 73.7°, and 15°, respectively. It can be seen that the experiments matches the simulation well.

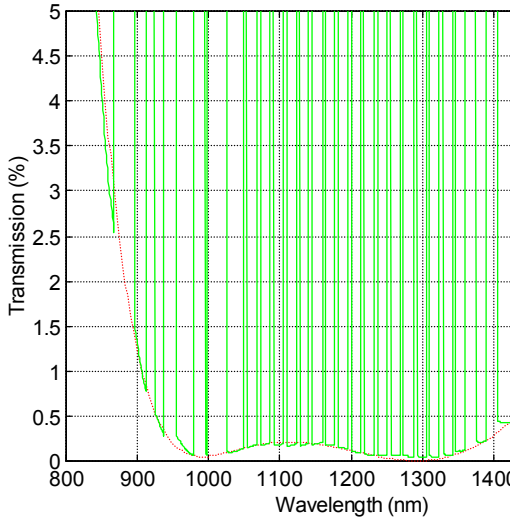

Fig.5. Theoretical and experimental comparison of the achromatic Half-wave switch

We have developed a data recover algorithm using Mathcad. The algorithm has the operation for Fourier transformation, incorporated the dispersion effect of the quartz which was measured experimentally. The recovered spectrum identifying the 1310-nm laser wavelength is shown in Figure 6. The broadened lineshape is due to the rough resolution of the 3-stage system (~145nm width).

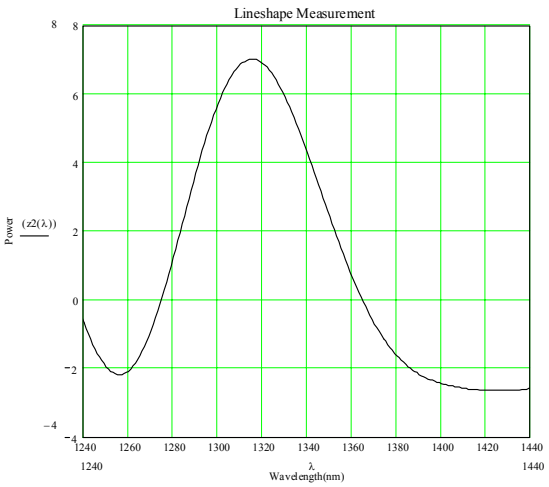

Figure 6. Measured and recovered spectrum of a laser source centered at 1310 nm.

IV. BROADBAND EOIFTS DESIGN

We are currently investigating the further development of a broadboard EOIFTS system. As shown in the previous depiction, the achromatic FLC switch band using 3 plates (2 NRF λ/2 retarders plus one FLC λ/2 switch) cannot cover the full range from 1 to 2.5 μm set in our original proposal. One possible solution proposed is by using two sets of achromatic switches at two different central wavelengths. This two-band solution results in system complexity as well as much higher cost.

However, the achromatic FLC switch band can be extended by using more plates. We modeled the spectral response and optical operation of a 5-plate achromatic half-wave switch working in the near-IR region using proprietary software modeling tools. The schematic of the achromatic half-wave solid-state switch is shown in Figure 7. Four passive Nitto Denko retardation film (NRF) sheets and one FLC switch are used to construct the compound retarder. The retardance for each NRF is a full-wave at 810 nm. The retardance of the FLC switch is a half-wave at 1550nm. An effective achromatic half-wave plate at 45° results from the structure where the orientations of the five waveplates are 7°, 36°, 102°, 36°, and 7°, respectively. The structure where the five orientations are 7°, 36°, 147°, 36°, and 7°, respectively, generates an effective achromatic half-wave plate at 0°.

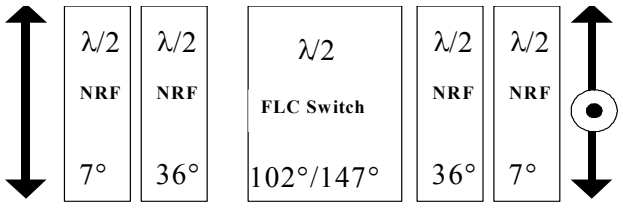

Figure 7. The Schematic of a super-achromatic half-wave switch

A typical simulation result for an effective achromatic half-wave plate at 45° (i.e. with the orientations of the five waveplates 7°, 36°, 102°, 36° and 7°, respectively) is shown in Figure 8. The spectral range with leakage less than 0.5% is from 1161 nm to 2413 nm. This"super-achromatic" design is close to the requirement from 1 to 2.5 μm. By optimizing the angle orientations, the super-band can be further improved (though still short of the perfect requirement from 1 to 2.5 μm). Figure 9 shows a result with the orientations of the five waveplates 7°, 35.8°, 101.5°, 35.8° and 7°, respectively. The spectral range with leakage less than 0.5% is from 1155 nm to 2437 nm.

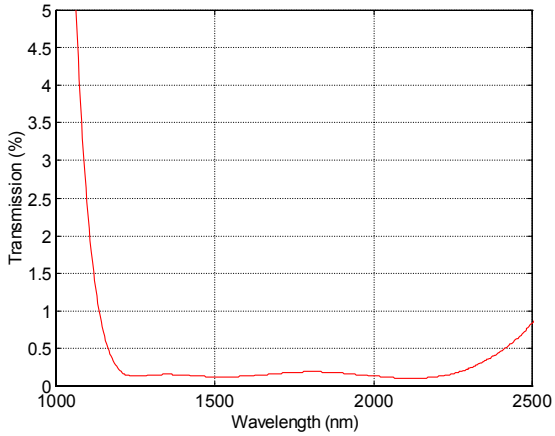

Figure 8. Simulation of the super-achromatic half-wave switch with the orientations of the five waveplates: 7°, 36°, 102°, 36° and 7°.

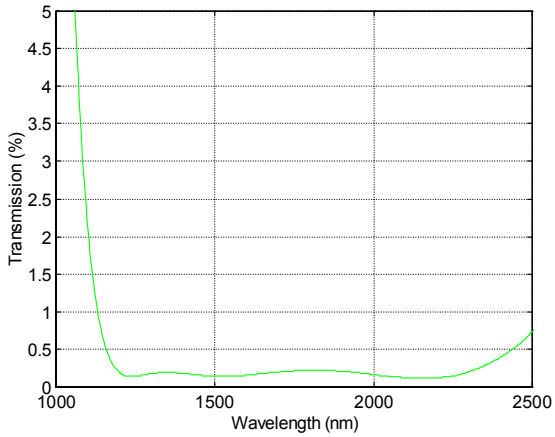

Figure 9. Simulation of the super-achromatic half-wave switch with the orientations of the five waveplates: 7°, 35.8°, 101.5°, 35.8° and 7°.

V. SUMMARY

We have developed principle of operation and system architecture of a electro-optic Fourier transform spectrometer. Initially, we have demonstrated a proof-of-principle 3-stage IR FTS breadboard. The major components design, fabrication and test results have been reported. The experimental result of spectral data capture

of that of a test diode laser source and the follow-on recovery through an inverse Fourier transform have also been accomplished. Future work includes the development phase retarders with of high birefringence material (e.g. YVO_4) to greatly reduced the system light path is underway. We will also develop a multiple stage system with ultrahigh resolution. Imaging optics will also be included into the system to enable hyperspectral imaging applications

ACKNOWLEDGMENT

The research described in this paper was carried out by the Jet Propulsion Laboratory, California Institute of Technology, under a contract with the National Aeronautics and Space Administration. The authors wish to express their sincere thanks to Dr. Geoffrey helpful technical discussions.

REFERENCES

[1] G. D. Sharp *et al.* "Polarization Interferometer Using Multi-order and Zero-order Birefringence Switches", U.S. Patent Application 08/948,860, Claims allowed (10/12/99).

[2] G. D. Sharp, P. Wang, S. Serati, T. Ewing, "Liquid Crystal Fourier Transform Spectrometer", SPIE AeroSense, (1998).

[3] P. Fellgett, Cambridge University thesis, 1951.

[4] G. D. Sharp, K. M. Johnson, "Liquid crystal achromatic compound retarder" , U. S. Patent 5,658,490

[5] Xiaowei Xia, Steve Serati, Teresa Ewing, Ping Wang, "A massively parallel liquid crystal Fourier transform spectrometer", Final report of Air Force Phase-II SBIR project, Dec. 1999.